Partial wave analysis of $J/\psi \to \gamma\eta\eta$

M. Ablikim,[1] M. N. Achasov,[6] O. Albayrak,[3] D. J. Ambrose,[39] F. F. An,[1] Q. An,[40] J. Z. Bai,[1] R. Baldini Ferroli,[17a] Y. Ban,[26] J. Becker,[2] J. V. Bennett,[16] N. Berger,[1] M. Bertani,[17a] J. M. Bian,[38] E. Boger,[19,*] O. Bondarenko,[20] I. Boyko,[19] R. A. Briere,[3] V. Bytev,[19] H. Cai,[44] X. Cai,[1] O. Cakir,[34a] A. Calcaterra,[17a] G. F. Cao,[1] S. A. Cetin,[34b] J. F. Chang,[1] G. Chelkov,[19,*] G. Chen,[1] H. S. Chen,[1] J. C. Chen,[1] M. L. Chen,[1] S. J. Chen,[24] X. Chen,[26] Y. B. Chen,[1] H. P. Cheng,[14] Y. P. Chu,[1] D. Cronin-Hennessy,[38] H. L. Dai,[1] J. P. Dai,[1] D. Dedovich,[19] Z. Y. Deng,[1] A. Denig,[18] I. Denysenko,[19,†] M. Destefanis,[43a,43c] W. M. Ding,[28] Y. Ding,[22] L. Y. Dong,[1] M. Y. Dong,[1] S. X. Du,[46] J. Fang,[1] S. S. Fang,[1] L. Fava,[43b,43c] C. Q. Feng,[40] P. Friedel,[2] C. D. Fu,[1] J. L. Fu,[24] O. Fuks,[19,*] Y. Gao,[33] C. Geng,[40] K. Goetzen,[7] W. X. Gong,[1] W. Gradl,[18] M. Greco,[43a,43c] M. H. Gu,[1] Y. T. Gu,[9] Y. H. Guan,[36] A. Q. Guo,[25] L. B. Guo,[23] T. Guo,[23] Y. P. Guo,[25] Y. L. Han,[1] F. A. Harris,[37] K. L. He,[1] M. He,[1] Z. Y. He,[25] T. Held,[2] Y. K. Heng,[1] Z. L. Hou,[1] C. Hu,[23] H. M. Hu,[1] J. F. Hu,[35] T. Hu,[1] G. M. Huang,[4] G. S. Huang,[40] J. S. Huang,[12] L. Huang,[1] X. T. Huang,[28] Y. Huang,[24] Y. P. Huang,[1] T. Hussain,[42] C. S. Ji,[40] Q. Ji,[1] Q. P. Ji,[25] X. B. Ji,[1] X. L. Ji,[1] L. L. Jiang,[1] X. S. Jiang,[1] J. B. Jiao,[28] Z. Jiao,[14] D. P. Jin,[1] S. Jin,[1] F. F. Jing,[33] N. Kalantar-Nayestanaki,[20] M. Kavatsyuk,[20] B. Kopf,[2] M. Kornicer,[37] W. Kuehn,[35] W. Lai,[1] J. S. Lange,[35] P. Larin,[11] M. Leyhe,[2] C. H. Li,[1] Cheng Li,[40] Cui Li,[40] D. M. Li,[46] F. Li,[1] G. Li,[1] H. B. Li,[1] J. C. Li,[1] K. Li,[10] Lei Li,[1] Q. J. Li,[1] S. L. Li,[1] W. D. Li,[1] W. G. Li,[1] X. L. Li,[28] X. N. Li,[1] X. Q. Li,[25] X. R. Li,[27] Z. B. Li,[32] H. Liang,[40] Y. F. Liang,[30] Y. T. Liang,[35] G. R. Liao,[33] X. T. Liao,[1] D. Lin,[11] B. J. Liu,[1] C. L. Liu,[3] C. Y. Liu,[1] C. X. Liu,[1] F. H. Liu,[29] Fang Liu,[1] Feng Liu,[4] H. Liu,[1] H. B. Liu,[9] H. H. Liu,[13] H. M. Liu,[1] H. W. Liu,[1] J. P. Liu,[44] K. Liu,[33] K. Y. Liu,[22] Kai Liu,[36] P. L. Liu,[28] Q. Liu,[36] S. B. Liu,[40] X. Liu,[21] Y. B. Liu,[25] Z. A. Liu,[1] Zhiqiang Liu,[1] Zhiqing Liu,[1] H. Loehner,[20] G. R. Lu,[12] H. J. Lu,[14] J. G. Lu,[1] Q. W. Lu,[29] X. R. Lu,[36] Y. P. Lu,[1] C. L. Luo,[23] M. X. Luo,[45] T. Luo,[37] X. L. Luo,[1] M. Lv,[1] C. L. Ma,[36] F. C. Ma,[22] H. L. Ma,[1] Q. M. Ma,[1] S. Ma,[1] T. Ma,[1] X. Y. Ma,[1] F. E. Maas,[11] M. Maggiora,[43a,43c] Q. A. Malik,[42] Y. J. Mao,[26] Z. P. Mao,[1] J. G. Messchendorp,[20] J. Min,[1] T. J. Min,[1] R. E. Mitchell,[16] X. H. Mo,[1] H. Moeini,[20] C. Morales Morales,[11] K. Moriya,[16] N. Yu. Muchnoi,[6] H. Muramatsu,[39] Y. Nefedov,[19] C. Nicholson,[36] I. B. Nikolaev,[6] Z. Ning,[1] S. L. Olsen,[27] Q. Ouyang,[1] S. Pacetti,[17b] M. Pelizaeus,[2] H. P. Peng,[40] K. Peters,[7] J. L. Ping,[23] R. G. Ping,[1] R. Poling,[38] E. Prencipe,[18] M. Qi,[24] S. Qian,[1] C. F. Qiao,[36] L. Q. Qin,[28] X. S. Qin,[1] Y. Qin,[26] Z. H. Qin,[1] J. F. Qiu,[1] K. H. Rashid,[42] G. Rong,[1] X. D. Ruan,[9] A. Sarantsev,[19,‡] B. D. Schaefer,[16] M. Shao,[40] C. P. Shen,[37,§] X. Y. Shen,[1] H. Y. Sheng,[1] M. R. Shepherd,[16] W. M. Song,[1] X. Y. Song,[1] S. Spataro,[43a,43c] B. Spruck,[35] D. H. Sun,[1] G. X. Sun,[1] J. F. Sun,[12] S. S. Sun,[1] Y. J. Sun,[40] Y. Z. Sun,[1] Z. J. Sun,[1] Z. T. Sun,[40] C. J. Tang,[30] X. Tang,[1] I. Tapan,[34c] E. H. Thorndike,[39] D. Toth,[38] M. Ullrich,[35] I. Uman,[34b] G. S. Varner,[37] B. Q. Wang,[26] D. Wang,[26] D. Y. Wang,[26] K. Wang,[1] L. L. Wang,[1] L. S. Wang,[1] M. Wang,[28] P. Wang,[1] P. L. Wang,[1] Q. J. Wang,[1] S. G. Wang,[26] X. F. Wang,[33] X. L. Wang,[40] Y. D. Wang,[17a] Y. F. Wang,[1] Y. Q. Wang,[18] Z. Wang,[1] Z. G. Wang,[1] Z. Y. Wang,[1] D. H. Wei,[8] J. B. Wei,[26] P. Weidenkaff,[18] Q. G. Wen,[40] S. P. Wen,[1] M. Werner,[35] U. Wiedner,[2] L. H. Wu,[1] N. Wu,[1] S. X. Wu,[40] W. Wu,[25] Z. Wu,[1] L. G. Xia,[33] Y. X. Xia,[15] Z. J. Xiao,[23] Y. G. Xie,[1] Q. L. Xiu,[1] G. F. Xu,[1] G. M. Xu,[26] Q. J. Xu,[10] Q. N. Xu,[36] X. P. Xu,[31] Z. R. Xu,[40] F. Xue,[4] Z. Xue,[1] L. Yan,[40] W. B. Yan,[40] Y. H. Yan,[15] H. X. Yang,[1] Y. Yang,[4] Y. X. Yang,[8] H. Ye,[1] M. Ye,[1] M. H. Ye,[5] B. X. Yu,[1] C. X. Yu,[25] H. W. Yu,[26] J. S. Yu,[21] S. P. Yu,[28] C. Z. Yuan,[1] Y. Yuan,[1] A. A. Zafar,[42] A. Zallo,[17a] S. L. Zang,[24] Y. Zeng,[15] B. X. Zhang,[1] B. Y. Zhang,[1] C. Zhang,[24] C. C. Zhang,[1] D. H. Zhang,[1] H. H. Zhang,[32] H. Y. Zhang,[1] J. Q. Zhang,[1] J. W. Zhang,[1] J. Y. Zhang,[1] J. Z. Zhang,[1] LiLi Zhang,[15] R. Zhang,[36] S. H. Zhang,[1] X. J. Zhang,[1] X. Y. Zhang,[28] Y. Zhang,[1] Y. H. Zhang,[1] Z. P. Zhang,[40] Z. Y. Zhang,[44] Zhenghao Zhang,[4] G. Zhao,[1] H. S. Zhao,[1] J. W. Zhao,[1] K. X. Zhao,[23] Lei Zhao,[40] Ling Zhao,[1] M. G. Zhao,[25] Q. Zhao,[1] S. J. Zhao,[46] T. C. Zhao,[1] X. H. Zhao,[24] Y. B. Zhao,[1] Z. G. Zhao,[40] A. Zhemchugov,[19,*] B. Zheng,[41] J. P. Zheng,[1] Y. H. Zheng,[36] B. Zhong,[23] L. Zhou,[1] X. Zhou,[44] X. K. Zhou,[36] X. R. Zhou,[40] C. Zhu,[1] K. Zhu,[1] K. J. Zhu,[1] S. H. Zhu,[1] X. L. Zhu,[33] Y. C. Zhu,[40] Y. M. Zhu,[25] Y. S. Zhu,[1] Z. A. Zhu,[1] J. Zhuang,[1] B. S. Zou,[1] and J. H. Zou[1]

(BESIII Collaboration)

[1]*Institute of High Energy Physics, Beijing 100049, People's Republic of China*
[2]*Bochum Ruhr-University, D-44780 Bochum, Germany*
[3]*Carnegie Mellon University, Pittsburgh, Pennsylvania 15213, USA*
[4]*Central China Normal University, Wuhan 430079, People's Republic of China*
[5]*China Center of Advanced Science and Technology, Beijing 100190, People's Republic of China*
[6]*G.I. Budker Institute of Nuclear Physics SB RAS (BINP), Novosibirsk 630090, Russia*
[7]*GSI Helmholtzcentre for Heavy Ion Research GmbH, D-64291 Darmstadt, Germany*
[8]*Guangxi Normal University, Guilin 541004, People's Republic of China*
[9]*GuangXi University, Nanning 530004, People's Republic of China*

[10]*Hangzhou Normal University, Hangzhou 310036, People's Republic of China*
[11]*Helmholtz Institute Mainz, Johann-Joachim-Becher-Weg 45, D-55099 Mainz, Germany*
[12]*Henan Normal University, Xinxiang 453007, People's Republic of China*
[13]*Henan University of Science and Technology, Luoyang 471003, People's Republic of China*
[14]*Huangshan College, Huangshan 245000, People's Republic of China*
[15]*Hunan University, Changsha 410082, People's Republic of China*
[16]*Indiana University, Bloomington, Indiana 47405, USA*
[17a]*INFN Laboratori Nazionali di Frascati, I-00044 Frascati, Italy*
[17b]*INFN and University of Perugia, I-06100 Perugia, Italy*
[18]*Johannes Gutenberg University of Mainz, Johann-Joachim-Becher-Weg 45, D-55099 Mainz, Germany*
[19]*Joint Institute for Nuclear Research, 141980 Dubna, Moscow region, Russia*
[20]*KVI, University of Groningen, NL-9747 AA Groningen, The Netherlands*
[21]*Lanzhou University, Lanzhou 730000, People's Republic of China*
[22]*Liaoning University, Shenyang 110036, People's Republic of China*
[23]*Nanjing Normal University, Nanjing 210023, People's Republic of China*
[24]*Nanjing University, Nanjing 210093, People's Republic of China*
[25]*Nankai University, Tianjin 300071, People's Republic of China*
[26]*Peking University, Beijing 100871, People's Republic of China*
[27]*Seoul National University, Seoul 151-747, Korea*
[28]*Shandong University, Jinan 250100, People's Republic of China*
[29]*Shanxi University, Taiyuan 030006, People's Republic of China*
[30]*Sichuan University, Chengdu 610064, People's Republic of China*
[31]*Soochow University, Suzhou 215006, People's Republic of China*
[32]*Sun Yat-Sen University, Guangzhou 510275, People's Republic of China*
[33]*Tsinghua University, Beijing 100084, People's Republic of China*
[34a]*Ankara University, Dogol Caddesi, 06100 Tandogan, Ankara, Turkey*
[34b]*Dogus University, 34722 Istanbul, Turkey*
[34c]*Uludag University, 16059 Bursa, Turkey*
[35]*Universitaet Giessen, D-35392 Giessen, Germany*
[36]*University of Chinese Academy of Sciences, Beijing 100049, People's Republic of China*
[37]*University of Hawaii, Honolulu, Hawaii 96822, USA*
[38]*University of Minnesota, Minneapolis, Minnesota 55455, USA*
[39]*University of Rochester, Rochester, New York 14627, USA*
[40]*University of Science and Technology of China, Hefei 230026, People's Republic of China*
[41]*University of South China, Hengyang 421001, People's Republic of China*
[42]*University of the Punjab, Lahore 54590, Pakistan*
[43a]*University of Turin, I-10125 Turin, Italy*
[43b]*University of Eastern Piedmont, I-15121 Alessandria, Italy*
[43c]*INFN, I-10125 Turin, Italy*
[44]*Wuhan University, Wuhan 430072, People's Republic of China*
[45]*Zhejiang University, Hangzhou 310027, People's Republic of China*
[46]*Zhengzhou University, Zhengzhou 450001, People's Republic of China*

(Received 31 December 2012; published 21 May 2013; corrected 24 May 2013)

Based on a sample of 2.25×10^8 J/ψ events collected with the BESIII detector at BEPCII, a full partial wave analysis on $J/\psi \to \gamma\eta\eta$ was performed using the relativistic covariant tensor amplitude method. The results show that the dominant 0^{++} and 2^{++} components are from the $f_0(1710)$, $f_0(2100)$, $f_0(1500)$, $f_2'(1525)$, $f_2(1810)$ and $f_2(2340)$. The resonance parameters and branching fractions are also presented.

DOI: 10.1103/PhysRevD.87.092009 PACS numbers: 13.25.Gv, 13.40.Hq, 14.40.Be

I. INTRODUCTION

Our present understanding of the strong interaction is based on a non-Abelian gauge field theory, quantum chromodynamics (QCD), which describes the interactions of quarks and gluons; it also predicts the existence of new types of hadrons with explicit gluonic degrees of freedom (e.g., glueballs, hybrids and multiquarks) [1–5]. These

*Also at the Moscow Institute of Physics and Technology, Moscow 141700, Russia.
†On leave from the Bogolyubov Institute for Theoretical Physics, Kiev 03680, Ukraine.
‡Also at the PNPI, Gatchina 188300, Russia.
§Present address: Nagoya University, Nagoya 464-8601, Japan.

unconventional states, if they exist, will enrich the meson spectroscopy greatly and shed light on the dynamics of QCD. According to lattice QCD predictions [6,7], the lowest mass glueball with $J^{PC} = 0^{++}$ is in the mass region from 1.5 to 1.7 GeV/c^2. However, the mixing of the pure glueball with nearby $q\bar{q}$ nonet mesons makes the identification of the glueballs difficult in both experiment and theory. Radiative J/ψ decay is a gluon-rich process and has long been regarded as one of the most promising hunting grounds for glueballs. In particular, for a J/ψ radiative decay to two pseudoscalar mesons, it offers a very clean laboratory to search for scalar and tensor glueballs because only intermediate states with $J^{PC} = \text{even}^{++}$ are possible. An early study of $J/\psi \to \gamma\eta\eta$ was made by the Crystal Ball Collaboration [8] with the first observation of $f_0(1710)$, but the study suffered from low statistics.

In this paper, the results of partial wave analysis (PWA) on $J/\psi \to \gamma\eta\eta$ are presented based on a sample of 2.25×10^8 J/ψ events [9] collected with the Beijing Spectrometer (BESIII) located at the upgraded Beijing Electron and Positron Collider (BEPCII) [10].

II. DETECTOR AND MONTE CARLO SIMULATION

The BESIII detector, described in detail in Ref. [11], has an effective geometrical acceptance of 93% of 4π. It contains a small cell helium-based main drift chamber (MDC) which provides momentum measurements of charged particles; a time-of-flight system (TOF) based on plastic scintillator which helps to identify charged particles; an electromagnetic calorimeter (EMC) made of CsI (Tl) crystals which is used to measure the energies of photons and provide trigger signals; and a muon system (MUC) made of resistive plate chambers (RPC). The momentum resolution of charged particles is 0.5% at 1 GeV/c in a 1 tesla magnetic field. The energy loss (dE/dx) measurement provided by the MDC has a resolution better than 6% for electrons from Bhabha scattering. The photon energy resolution can reach 2.5% (5%) at 1.0 GeV in the barrel (end caps) of the EMC. And the time resolution of TOF is 80 ps in the barrel and 110 ps in the end caps.

Monte Carlo (MC) simulated events are used to determine the detection efficiency, optimize the selection criteria, and study the possible backgrounds. The simulation of the BESIII detector, where the interactions of the particles with the detector material are simulated, is GEANT4 [12] based. The J/ψ resonance is produced with KKMC [13,14], while the subsequent decays are generated with EVTGEN [15]. The study of the background is based on a MC sample of 2.25×10^8 J/ψ inclusive decays which are generated with known branching fractions taken from the Particle Data Group (PDG) [16], or with LUNDCHARM [17] for the unmeasured decays.

III. EVENT SELECTION

In this analysis, the η meson is detected in its $\gamma\gamma$ decay. Each candidate event is required to have five or six good photons and no charged tracks. The photon candidates are selected from the showers in the EMC with deposited energy in the EMC barrel region ($|\cos\theta| < 0.8$) and EMC end cap region ($0.86 < |\cos\theta| < 0.92$) greater than 25 and 50 MeV, respectively. The energy deposit in nearby TOF counters is included to improve the reconstruction efficiency and energy resolution.

To suppress the background events with π^0 (e.g., $J/\psi \to \gamma\pi^0\pi^0$), the events that satisfy $|M_{\gamma\gamma} - m_{\pi^0}| < 0.015$ GeV/c^2 are removed, where $M_{\gamma\gamma}$ is the invariant mass of any pair of photon candidates and m_{π^0} is the nominal π^0 mass [16]. Then a four-constraint kinematic fit (4C), imposing energy-momentum conservation, is performed under the $J/\psi \to 5\gamma$ hypothesis to reduce background events and improve the mass resolution, and χ^2_{4C} is required to be less than 50. If the number of selected photons is larger than five, the fit is repeated using all permutation of the photons, and the combination with the smallest χ^2_{4C} is selected.

To distinguish the photons from η decays, a variable δ, defined as $\delta = \sqrt{(M_{\gamma_1\gamma_2} - m_\eta)^2 + (M_{\gamma_3\gamma_4} - m_\eta)^2}$, is introduced, and the combination with the minimum value of δ is chosen. The scatter plot of the invariant mass of one η candidate versus the other is shown in Fig. 1(a), where the decay $J/\psi \to \gamma\eta\eta$ is clear. In order to select a clean sample, both $M_{\gamma_1\gamma_2}$ and $M_{\gamma_3\gamma_4}$ are required to be in the η mass region, $|M_{\gamma_1\gamma_2}(M_{\gamma_3\gamma_4}) - m_\eta| < 0.04$ GeV/c^2, with m_η the nominal η mass [16]. The projection of $M(\gamma_1\gamma_2)$ [or $M(\gamma_3\gamma_4)$] with $M(\gamma_3\gamma_4)$ [or $M(\gamma_1\gamma_2)$] in the η mass region, is shown in Fig. 1(b). The mass resolution for m_η is about 10 MeV/c^2.

MC study shows that after the above selection, about 5.3% of events have a miscombination of photons, which mainly occurs between the radiative photon and one photon from an η. Therefore, a candidate event must have only one combination with $\delta < 0.05$ GeV/c^2 to remove these events, which reduces the fraction of events with a miscombination of photons to be 0.8%.

After that, clear diagonal bands, which correspond to the structures observed in the $\eta\eta$ invariant mass spectrum, can be seen in the Dalitz plot for the selected $J/\psi \to \gamma\eta\eta$ candidate events [Fig. 1(c)]. A further requirement on $M_{\gamma\eta}$, $|M_{\gamma\eta} - m_\phi| > 30$ MeV/c^2 is used to reject background events from $J/\psi \to \phi\eta(\phi \to \gamma\eta)$. Figure 1(d) shows the $\eta\eta$ invariant mass spectrum of the surviving 5460 events after the event selection. The selection efficiency is determined from a sample of phase space Monte Carlo events, with projections shown in Figs. 2(a)–2(c).

Potential background events have been studied using both MC and data samples. The non-η events are determined from the two-dimensional η mass sidebands,

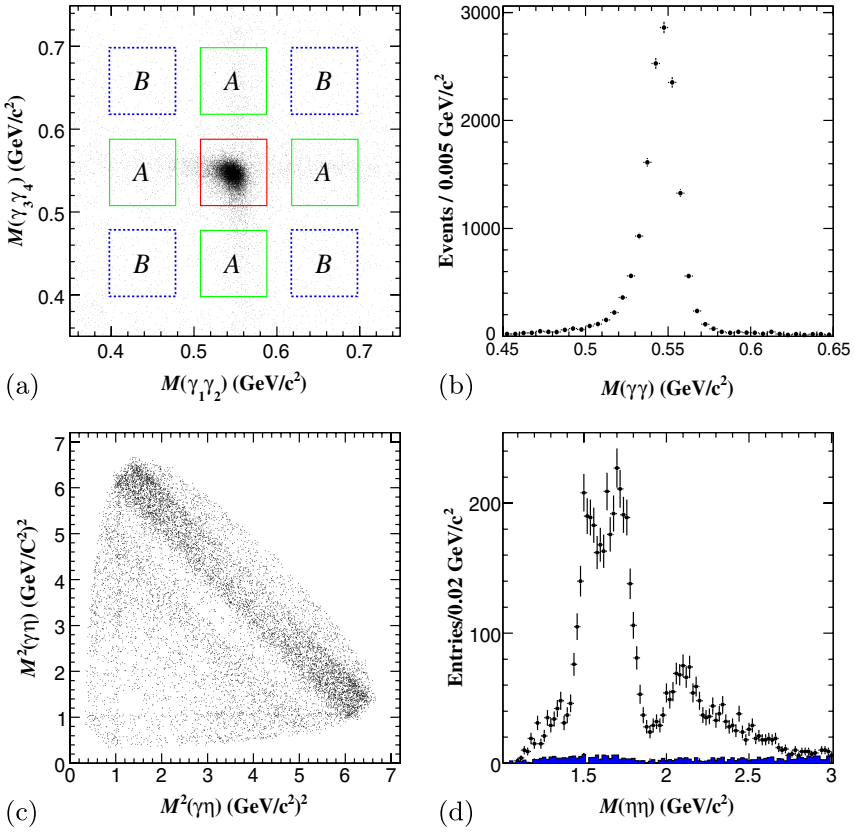

FIG. 1 (color online). (a) The scatter plot of $M_{\gamma_1\gamma_2}$ versus $M_{\gamma_3\gamma_4}$ after selecting candidates with the minimum δ (two entries/event). The two-dimensional η sidebands are framed in regions A and B. (b) $M(\gamma_1\gamma_2)$ [or $M(\gamma_3\gamma_4)$] with $M(\gamma_3\gamma_4)$ [or $M(\gamma_1\gamma_2)$] in the signal region. (c) Dalitz plot (two entries/event), before $\phi \to \gamma\eta$ veto. (d) The invariant mass spectrum of $\eta\eta$. The dots with error bars are data, and the shaded histogram is background estimated from η sidebands.

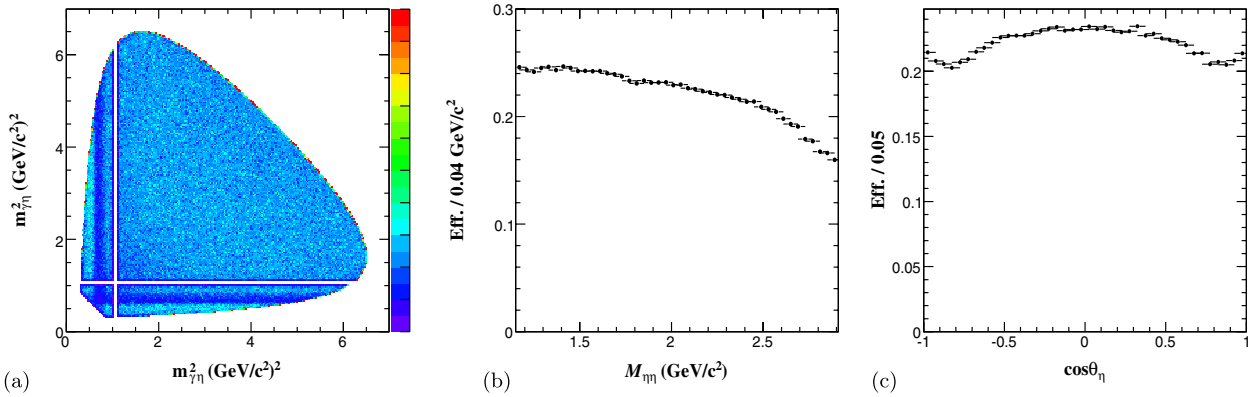

FIG. 2 (color online). The selection efficiency projected (a) on the Dalitz plot, (b) on the $\eta\eta$ mass distribution, (c) on the $\cos\theta_\eta$ angular distribution; θ_η is the polar angle of η in the $\eta\eta$ helicity frame.

$0.07\ \text{GeV}/c^2 < |M_{\gamma\gamma} - m_\eta| < 0.15\ \text{GeV}/c^2$, which are defined as frames A and B in Fig. 1(a). The shaded histogram in Fig. 1(d) shows the sideband events normalized according to $J/\psi \to 5\gamma$ phase space MC. In addition, the background events are studied with a MC sample of 225 million J/ψ inclusive events, and the main background events are found to be from $J/\psi \to \gamma\eta\pi^0\pi^0$ and $\gamma\pi^0\eta$. In this paper, the background events estimated from η mass sidebands, corresponding to a background level of 6%, are used in the partial wave analysis below.

IV. PARTIAL WAVE ANALYSIS

A. Analysis method

With GPUPWA, a partial wave analysis framework harnessing GPU parallel computing [18], a PWA was

performed to disentangle the structures present in $J/\psi \to \gamma\eta\eta$ decays. The quasi-two-body decay amplitudes in the sequential decay process $J/\psi \to \gamma X$, $X \to \eta\eta$ are constructed using covariant tensor amplitudes described in Ref. [19]. For J/ψ radiative decay to mesons, the general form for covariant tensor amplitude is

$$A = \psi_\mu(m_1) e^*_\nu(m_2) A^{\mu\nu} = \psi_\mu(m_1) e^*_\nu(m_2) \Sigma_i \Lambda_i U_i^{\mu\nu}, \quad (1)$$

where $\psi_\mu(m_1)$ is the J/ψ polarization four-vector, $e_\nu(m_2)$ is the polarization vector of the photon and $U_i^{\mu\nu}$ is the partial wave amplitude with coupling strength determined by a complex parameter Λ_i. The partial wave amplitudes U_i for the intermediate states used in the analysis are constructed with the four-momenta of daughter particles, and their specific expressions are given in Ref. [19].

For an intermediate resonance, the corresponding Breit-Wigner propagator is described by a function:

$$\mathrm{BW}(s) = \frac{1}{M^2 - s - iM\Gamma}, \quad (2)$$

where s is the invariant mass squared of daughter particles, and M and Γ are the mass and width of the intermediate resonance.

The relative magnitudes and phases of the amplitudes are determined by an unbinned maximum likelihood fit. The resonance parameters are optimized by the scan method: repeating the fits iteratively with various masses and widths until the optimized likelihood values converge. For the tensor states, the relative phases between three amplitudes for a certain resonance are theoretically expected to be very small [20]; therefore the relative phases of the three amplitudes for each tensor are set to zero in the fit so as to constrain the intensities further.

The basis of the likelihood fitting is that a hypothesized probability density function (PDF) would produce the data set under consideration. The probability to observe the event characterized by the measurement ξ is

$$P(\xi) = \frac{\omega(\xi)\epsilon(\xi)}{\int d\xi \omega(\xi)\epsilon(\xi)}, \quad (3)$$

where $\epsilon(\xi)$ is the detection efficiency and $\omega(\xi) \equiv \frac{d\sigma}{d\Phi}$ is the differential cross section, and $d\Phi$ is the standard element of phase space. The full differential cross section is

$$\frac{d\sigma}{d\Phi} = \left| \sum_j A_j \right|^2 = |A(V\eta) + A(0^{++}) + A(2^{++}) + A(4^{++}) + \cdots|^2, \quad (4)$$

where $A(J^{\mathrm{PC}})$ is the full amplitude for all resonances whose spin-parities are J^{PC}, and $A(V\eta)$ is the contribution of the sequential decay processes such as $J/\psi \to \phi\eta \to \gamma\eta\eta$. $\int d\xi \omega(\xi)\epsilon(\xi) \equiv \sigma'$ is the measured total cross section.

The joint probability density for observing the N events in the data sample is

$$\mathcal{L} = \prod_{i=1}^{N} P(\xi_i) = \prod_{i=1}^{N} \frac{\left(\frac{d\sigma}{d\Phi}\right)_i \epsilon(\xi_i)}{\sigma'}. \quad (5)$$

For the technical reasons, rather than maximizing $\mathcal{L}$, $\mathcal{S} = -\ln \mathcal{L}$ is minimized, i.e.,

$$\ln \mathcal{L} = \sum_{i=1}^{N} \ln \left(\frac{\left(\frac{d\sigma}{d\Phi}\right)_i}{\sigma'} \right) + \sum_{i=1}^{N} \ln \epsilon(\xi_i), \quad (6)$$

for a given data set; the second term is a constant and has no impact on the determination of the parameters of the amplitudes or on the relative changes of $\mathcal{S}$ values. So, for the fitting, $\ln \mathcal{L}$ defined as

$$\ln \mathcal{L} = \sum_{i=1}^{N} \ln \left(\frac{\left(\frac{d\sigma}{d\Phi}\right)_i}{\sigma'} \right) = \sum_{i=1}^{N} \ln \left(\frac{d\sigma}{d\Phi}\right)_i - N \ln \sigma', \quad (7)$$

is used. The free parameters are optimized by FUMILI [21]. The measured total cross section σ' is evaluated using MC techniques. Namely, a MC sample of N_{gen} is generated with signal events that are distributed uniformly in phase space. These events are subjected to our selection criteria and yield a sample of N_{acc} accepted events. The normalization integral is computed as

$$\int d\xi \omega(\xi)\epsilon(\xi) = \sigma' \to \frac{1}{N_{\mathrm{acc}}} \sum_{k}^{N_{\mathrm{acc}}} \left(\frac{d\sigma}{d\Phi}\right)_k. \quad (8)$$

The background contribution is estimated with η sidebands. In the log-likelihood calculation, the likelihood values of η sideband events are given negative weights, and are removed from data since the log-likelihood value of data is the sum of the log-likelihood values of signal and background events, i.e.,

$$\mathcal{S} = -(\ln \mathcal{L}_{\mathrm{DATA}} - \ln \mathcal{L}_{\mathrm{BG}}). \quad (9)$$

The number of the fitted events N_X for an intermediate resonance X, which has N_W independent partial wave amplitudes A_i, is defined as

$$N_X = \frac{\sigma_X}{\sigma'} \cdot N', \quad (10)$$

where N' is the number of selected events after background subtraction, and

$$\sigma_X = \frac{1}{N_{\mathrm{acc}}} \sum_{k}^{N_{\mathrm{acc}}} \left| \sum_{j}^{N_W} (A_j)_k \right|^2 \quad (11)$$

is the measured cross section of the resonance X and is calculated with the same MC sample as the measured total cross section σ'.

The branching ratio of $J/\psi \to \gamma X$, $X \to \eta\eta$ is calculated with

$$\mathcal{B}(J/\psi \to \gamma X \to \gamma\eta\eta) = \frac{N_X}{N_{J/\psi} \cdot \varepsilon_X \cdot \mathcal{B}^2_{\eta\to\gamma\gamma}}, \quad (12)$$

where the detection efficiency ε_X is obtained by the partial wave amplitude weighted MC sample,

$$\varepsilon_X = \frac{\sigma_X}{\sigma_X^{\rm gen}} = \frac{\sum_k^{N_{\rm acc}} \left| \sum_j^{N_W} (A_j)_k \right|^2}{\sum_i^{N_{\rm gen}} \left| \sum_j^{N_W} (A_j)_i \right|^2}. \quad (13)$$

The statistical errors for masses, widths and branching ratios in a PWA are defined as one standard deviation from the optimized results, which corresponds to a change, 0.5, of the log-likelihood value for a specific parameter. In this analysis, the changes of log-likelihood value and the number of free parameters in the fit with or without a resonance are used to evaluate the statistical significance of this resonance.

B. PWA results

In this analysis, all possible combinations of 0^{++}, 2^{++}, 4^{++} resonances listed in the PDG summary table [22] are evaluated, and the fitted components with statistical significance larger than 5.0σ are kept as the basic solution. The contribution from 4^{++} [$f_4(2050)$] with a statistical significance of 0.4σ is ignored. There are six resonances, $f_0(1500)$, $f_0(1710)$, $f_0(2100)$, $f_2'(1525)$, $f_2(1810)$, $f_2(2340)$, as well as 0^{++} phase space and $J/\psi \to \phi\eta$ included in the basic solution. Although most of the $J/\psi \to \phi\eta$ events have been rejected by the above ϕ mass window requirement, $J/\psi \to \phi\eta$ is included in the PWA to evaluate its impact from the interference between the tail of ϕ and other components from $J/\psi \to \gamma X(X \to \eta\eta)$. The masses and widths of the resonances, branching ratios of J/ψ radiative decaying to X and the statistical significances are summarized in Table I.

The comparisons of the $\eta\eta$ invariant mass spectrum, $\cos\theta_\eta$, $\cos\theta_\gamma$ and ϕ_η distributions between the data and the PWA fit projections (weighted by MC efficiencies) are displayed in Figs. 3(a)–3(d), where θ_γ is the polar angle of the radiative photon in the J/ψ rest frame, and θ_η and ϕ_η are the polar angle and azimuthal angle of η in the $\eta\eta$ helicity frame. The PWA results provide a good description of data. To illustrate the contributions from each component, the projections for each specific resonance are plotted [Figs. 4(a)–4(f): $f_0(1500)$, $f_0(1710)$, $f_0(2100)$, $f_2'(1525)$, $f_2(1810)$, $f_2(2340)$], 0^{++} phase space [Fig. 4(g)], total 0^{++} component [Fig. 4(h)] and total 2^{++} component [Fig. 4(i)], where the dots with error bars are data with the background events subtracted and the solid histograms are the projections of the PWA for the specific components.

1. Scalar components

The histogram in Fig. 4(h) shows the contribution of all the scalar components, where the dominant ones are from $f_0(1710)$ and $f_0(2100)$. For the $f_0(1710)$ meson, the PWA gives a mass of 1759 ± 6 MeV/c^2 and a width of 172 ± 10 MeV/c^2 with a statistical significance of 25σ; the mass and width are consistent with those obtained from $J/\psi \to \gamma K\bar{K}$ [23] and $J/\psi \to \gamma\pi\pi$ [24] at BESII. The $f_0(2100)$ is observed with a statistical significance of 13.9σ, and its mass and width are determined to be 2081 ± 13 MeV/c^2 and 273^{+27}_{-24} MeV/c^2, respectively, which are in agreement with previous measurements [25–28]. The product branching fractions of the $f_0(1710)$ and $f_0(2100)$ are measured to be $\mathcal{B}(J/\psi \to \gamma f_0(1710) \to \gamma\eta\eta) = (2.35^{+0.13}_{-0.11}) \times 10^{-4}$ and $\mathcal{B}(J/\psi \to \gamma f_0(2100) \to \gamma\eta\eta) = (1.13^{+0.09}_{-0.10}) \times 10^{-4}$, where the errors are statistical only.

The $f_0(1500)$ is observed with a statistical significance of 8.2σ, but its production rate, $\mathcal{B}(J/\psi \to \gamma f_0(1500) \to \gamma\eta\eta) = (1.65^{+0.26}_{-0.31}) \times 10^{-5}$, is about one order of magnitude lower than that of $f_0(1710)$ and $f_0(2100)$ since its dominant decay modes are 4π and $\pi\pi$ [16]. The mass and width obtained from the global fit are 1468^{+14}_{-15} MeV/c^2 and 136^{+41}_{-26} MeV/c^2, respectively, which are consistent with the BESII measurements in $J/\psi \to \gamma\pi\pi$ [24].

The first experimental evidence for the $f_0(1790)$ ($M = 1790^{+40}_{-30}$ MeV/c^2 and $\Gamma = 270^{+60}_{-30}$ MeV/c^2) was observed in $J/\psi \to \phi\pi\pi$ [29]. Of interest is that no evidence was observed in $J/\psi \to \phi K\bar{K}$ [29]. In this analysis, if the dominant $f_0(1710)$ in the basic solution is replaced with $f_0(1790)$, the log-likelihood is worse by 30. If the $f_0(1790)$ is included as an additional resonance in the fit, the significance of $f_0(1790)$ is only 1.8σ, which indicates that the uncoupled $f_0(1790)$ is either suppressed in radiative decays or not coupled strongly to $\eta\eta$.

TABLE I. Summary of the PWA results, including the masses and widths for resonances, branching ratios of $J/\psi \to \gamma$X, as well as the significance. The first errors are statistical and the second ones are systematic. The statistical significances here are obtained according to the changes of the log-likelihood.

Resonance	Mass (MeV/c^2)	Width (MeV/c^2)	$\mathcal{B}(J/\psi \to \gamma X \to \gamma\eta\eta)$	Significance
$f_0(1500)$	1468^{+14+23}_{-15-74}	$136^{+41+28}_{-26-100}$	$(1.65^{+0.26+0.51}_{-0.31-1.40}) \times 10^{-5}$	8.2σ
$f_0(1710)$	$1759 \pm 6^{+14}_{-25}$	$172 \pm 10^{+32}_{-16}$	$(2.35^{+0.13+1.24}_{-0.11-0.74}) \times 10^{-4}$	25.0σ
$f_0(2100)$	$2081 \pm 13^{+24}_{-36}$	273^{+27+70}_{-24-23}	$(1.13^{+0.09+0.64}_{-0.10-0.28}) \times 10^{-4}$	13.9σ
$f_2'(1525)$	$1513 \pm 5^{+4}_{-10}$	75^{+12+16}_{-10-8}	$(3.42^{+0.43+1.37}_{-0.51-1.30}) \times 10^{-5}$	11.0σ
$f_2(1810)$	1822^{+29+66}_{-24-57}	$229^{+52+88}_{-42-155}$	$(5.40^{+0.60+3.42}_{-0.67-2.35}) \times 10^{-5}$	6.4σ
$f_2(2340)$	$2362^{+31+140}_{-30-63}$	$334^{+62+165}_{-54-100}$	$(5.60^{+0.62+2.37}_{-0.65-2.07}) \times 10^{-5}$	7.6σ

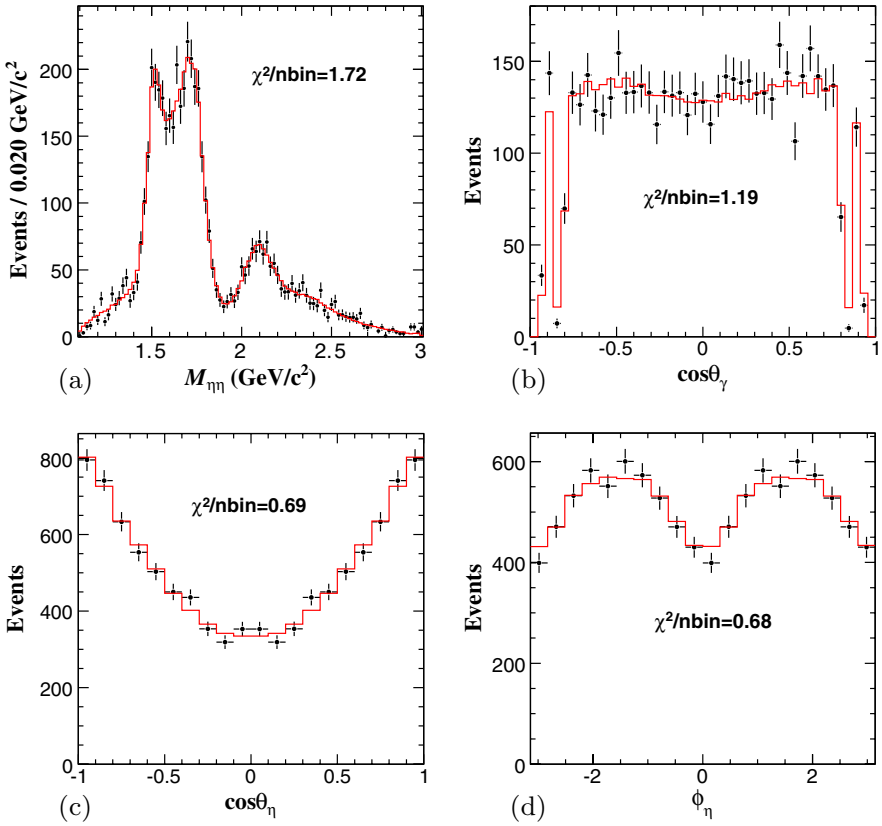

FIG. 3 (color online). Comparisons between data and PWA fit projections: (a) the invariant mass spectrum of $\eta\eta$, (b)–(c) the polar angle of the radiative photon in the J/ψ rest frame and η in the $\eta\eta$ helicity frame [the gaps in (b) are due to the photon selection], (d) the azimuthal angle of η in the $\eta\eta$ helicity frame. The black dots with error bars are data with background subtracted, and the solid histograms show the PWA projections.

To evaluate the contributions from other scalar mesons, $f_0(1370)$, $f_0(2020)$, $f_0(2200)$ and $f_0(2330)$, the PWA was performed including them, and none of them has significance greater than 5.0σ. Therefore, they are not included in the basic solution.

2. Tensor components

The total contribution from the tensor components is shown as the histogram in Fig. 4(i), where the peak around 1.5 GeV/c^2 is dominated by the well-established resonance $f_2'(1525)$ and the tensor components contributing to the bump around 2.1 GeV/c^2 are from $f_2(1810)$ and $f_2(2340)$. The fitted mass and width of $f_2'(1525)$ are 1513 ± 5 MeV/c^2 and 75^{+12}_{-10} MeV/c^2, respectively, which are consistent with the world average values [16], and the product branching fraction is calculated to be $\mathcal{B}(J/\psi \to \gamma f_2'(1525) \to \gamma\eta\eta) = (3.42^{+0.43}_{-0.51}) \times 10^{-5}$. If $f_2'(1525)$ is replaced with another tensor meson close to 1.5 GeV/c^2, $f_2(1565)$, the log-likelihood is worse by 18. The PWA is also performed including $f_2(1565)$ as an additional resonance, and its statistical significance is only 2.0σ.

The global fit shows that there is a tensor component around 1.8 GeV/c^2 with a statistical significance of 6.4σ, and its mass and width are determined to be 1822^{+29}_{-24} MeV/c^2 and 229^{+52}_{-42} MeV/c^2, respectively, which is likely to be the $f_2(1810)$. However the changes of the log-likelihood value are only 0.8 or 0.7, if we replace it with the $f_2(1910)$ or $f_2(1950)$, respectively, using the world average values for their masses and widths [16], which indicates that we cannot distinguish it from $f_2(1810)$, $f_2(1910)$ and $f_2(1950)$ with the present statistics. In this analysis, this tensor component is denoted as $f_2(1810)$, and the ambiguous assignment of $f_2(1810)$ or $f_2(1950)$ is considered as a source of systematic error.

To investigate contributions from other possible tensor resonances, $f_2(2010)$, $f_2(2150)$, $f_J(2220)$, $f_2(2300)$ and $f_2(2340)$, the fits were performed with alternative combinations, and the statistical significances of $f_2(2010)$, $f_2(2150)$ and $f_J(2220)$ are all less than 5.0σ, and the best fit favors the presence of $f_2(2340)$ (the statistical significance is 7.6σ) with a mass of 2362^{+31}_{-30} MeV/c^2, a width of 334^{+62}_{-54} MeV/c^2, and a product branching fraction of $\mathcal{B}(J/\psi \to \gamma f_2(2340) \to \gamma\eta\eta) = (5.60^{+0.62}_{-0.65}) \times 10^{-5}$. Since the mass of $f_2(2300)$ is close to $f_2(2340)$, an attempt was made to replace $f_2(2340)$ with $f_2(2300)$ by fixing its mass and width to those in PDG [16], and the log-likelihood value is worse by 15. The narrow $f_J(2220)$ [also known as $\xi(2230)$], which was reported by MarkIII [30] and

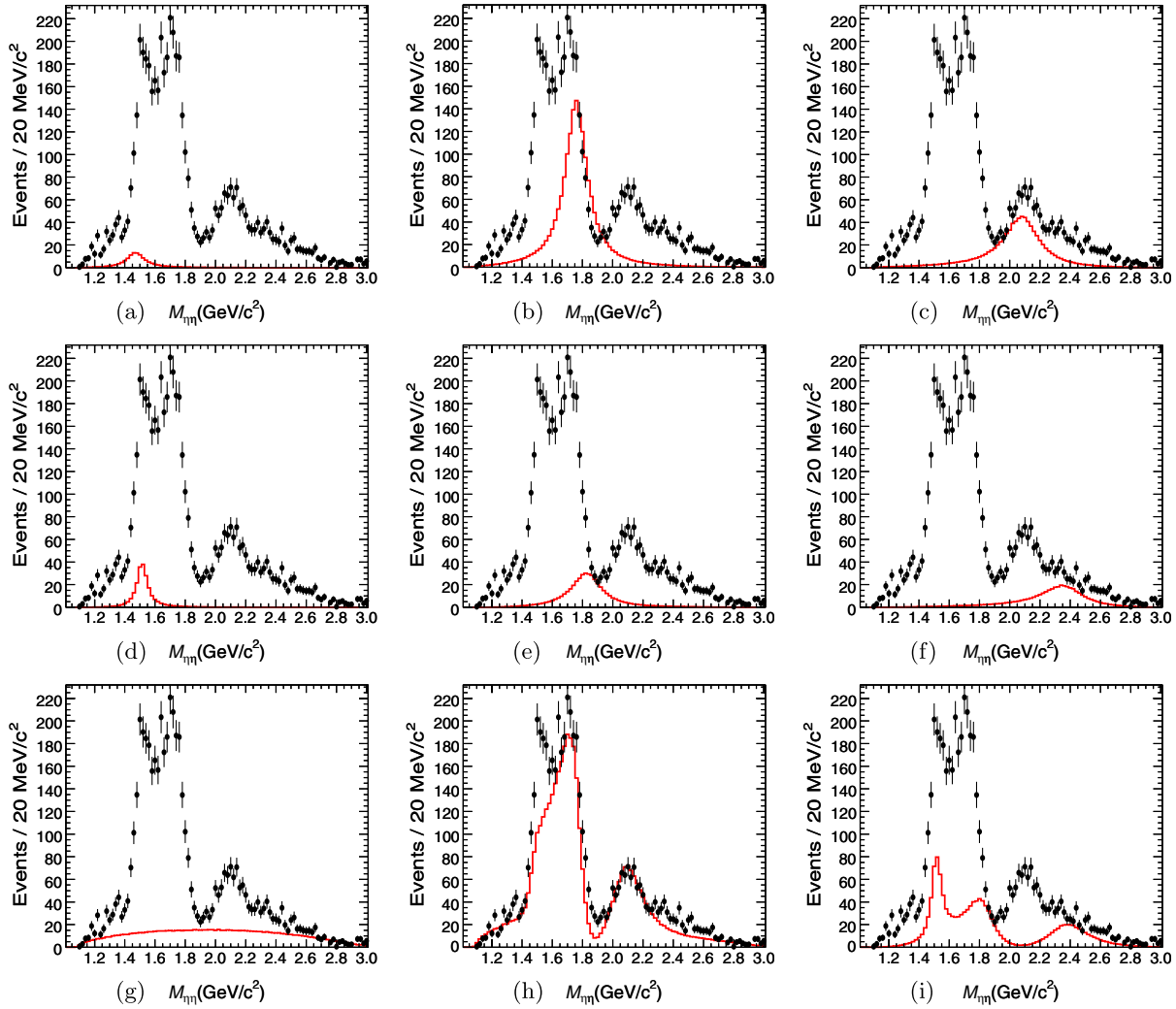

FIG. 4 (color online). Contribution of the components. (a) $f_0(1500)$, (b) $f_0(1710)$, (c) $f_0(2100)$, (d) $f_2'(1525)$, (e) $f_2(1810)$, (f) $f_2(2340)$, (g) 0^{++} phase space, (h) total 0^{++} component, and (i) total 2^{++} component. The dots with error bars are data with background subtracted, and the solid histograms are the projection of the PWA.

BES [31], is also studied. In this analysis no evident narrow peak around 2.2 GeV/c^2 over the broad bump is observed in the $\eta\eta$ mass spectrum shown in Fig. 1(d). When the $f_J(2220)$ is included in the PWA, the statistical significance is found to be 0.4σ.

3. Nonresonant contribution and $J/\psi \to \phi\eta$

In the analysis, the nonresonant contribution in the decay $J/\psi \to \gamma\eta\eta$ is described with 0^{++} phase space, with a statistical significance of 12.4σ, and the product branching fraction is calculated to be $(1.47^{+0.01}_{-0.02}) \times 10^{-4}$. An alternative fit is made by replacing the 0^{++} phase space with 2^{++} phase space, and the log-likelihood value is worse by 30. In addition to 0^{++} phase space, a 2^{++} phase space component to describe the nonresonant contribution was used, but the significance of the additional 2^{++} phase space is less than 4.0σ. The impact from the uncertainty of the nonresonant contribution is taken as a source of systematic error.

V. SYSTEMATIC ERROR

The systematic sources and their corresponding contributions to the measurements of mass, width and branching fractions are described below.

(i) Background uncertainty. The background events estimated with the η mass sidebands are included in the global fit with negative weights. To estimate the systematic error, the global fit was done with background events from different η mass sideband regions, and the changes of results are assigned as the systematic errors.

(ii) Uncertainty from extra components. As mentioned above, possible extra 0^{++}, 2^{++} and 4^{++} components with low significance were removed from the global fit. The changes of results caused by including them in the global fit are assigned as the systematic errors.

(iii) Uncertainty from resonance parameters. To estimate the impact of one specific resonance on the

TABLE II. Summary of the systematic errors from the event selection.

Error sources	Systematic error (%)
Photon efficiency	5.0
Kinematic fit	6.5
η selection	0.8
Number of J/ψ events	1.24
Total	8.3

others, the optimized mass and width of each resonance were varied by one standard deviation (statistical error only), and then the global fit was redone. The differences between the results with and without the variation of the resonance parameters are assigned as the systematic errors. As discussed above, the $f_2(1810)$ cannot be distinguished from $f_2(1910)$ or $f_2(1950)$. Therefore the fits were redone fixing the mass and width to be the values of $f_2(1810)$ and $f_2(1950)$ in PDG [16], respectively, and the maximum changes of the results are regarded as the systematic uncertainties.

(iv) To estimate the uncertainty from $J/\psi \to \phi\eta$, an alternative fit was performed without the contribution of $J/\psi \to \phi\eta$, and the changes of results are taken as the systematic errors.

(v) Mass resolution. In the global fit, the mass resolution is not considered to simplify the analysis. In order to estimate its possible impact on the fitted resonance parameters, a test was made by smearing the line shape of each resonance from the global fit with the corresponding mass resolution obtained from MC simulation. The impact on a resonance with a width greater than 100 MeV/c^2 is less than 2%, which is negligible compared with uncertainties from other sources. For $f_2'(1525)$, the width is smeared by 5 MeV/c^2 with respect to the PWA result 75^{+12}_{-10}(stat) MeV/c^2. The difference is considered as a source of systematic error to the width measurement.

(vi) Phase space description. The uncertainty from the description of the nonresonant contribution is estimated from an alternative fit by including both 0^{++} and 2^{++} phase space.

(vii) Breit-Wigner formula. The changes of the fit results caused by replacing the constant width Breit-Wigner with a kinematic dependent width Breit-Wigner [32] are taken as the uncertainties from different resonance parametrizations.

In addition to the above systematic sources, the systematic errors from the event selection criteria, trigger efficiency and the number of J/ψ events, which are summarized in Table II, are also included in the branching fraction measurements.

(i) Photon detection. For the decay mode analyzed in this paper, five photons are involved in the final states. The uncertainty due to photon detection and photon conversion is 1% per photon. This is determined from studies of photon detection efficiencies in well understood decays such as $J/\psi \to \rho^0\pi^0$ and study of photon conversion via $e^+e^- \to \gamma\gamma$ [33,34].

(ii) Trigger efficiency. The trigger efficiency of the BESIII detector was found to be very close to 100% from studies using different samples selected from J/ψ or $\psi(2S)$ decays. Therefore, the trigger efficiency is assumed to be 100% in the calculation of the branching fractions, and the systematic error from this source is neglected.

(iii) Kinematic fit and η selection. The systematic error from the kinematic fit is studied with the clean channel $\psi' \to \gamma\chi_{c0}$ ($\chi_{c0} \to \eta\eta$), as described in Ref. [34]. The efficiency is defined as the ratio of χ_{c0} yield with and without the kinematic requirement of $\chi^2_{4C} < 50$, where the χ_{c0} yield is obtained by fitting the $\eta\eta$ mass spectrum with the MC signal shape and a second-order polynomial. The difference between data and MC simulation, 6.5%,

TABLE III. Summary of the systematic error sources and their corresponding contributions to masses and widths of the resonances X (MeV/c^2), which are denoted as ΔM and $\Delta\Gamma$, respectively.

	$f_0(1500)$		$f_2'(1525)$		$f_0(1710)$		$f_2(1810)$		$f_0(2100)$		$f_2(2340)$	
Systematic error	ΔM	$\Delta\Gamma$	ΔM	$\Delta\Gamma$	ΔM	$\Delta\Gamma$	ΔM	$\Delta\Gamma$	ΔM	$\Delta\Gamma$	ΔM	$\Delta\Gamma$
Background uncertainty	$^{+18}_{-8}$	-46	$+1$	$^{+6}_{-4}$	$^{+11}_{-13}$	$^{+19}_{-8}$	$^{+55}_{-39}$	$^{+61}_{-4}$	$^{+19}_{-32}$	$+38$	$+93$	$^{+43}_{-41}$
Extra resonances	$^{+9}_{-73}$	$^{+7}_{-84}$	$^{+2}_{-9}$	$^{+10}_{-4}$	$^{+8}_{-18}$	$^{+19}_{-11}$	$^{+19}_{-36}$	$^{+16}_{-141}$	$^{+7}_{-9}$	$^{+50}_{-4}$	$^{+76}_{-9}$	$^{+7}_{-2}$
Resonance parameters	$^{+11}_{-12}$	$^{+27}_{-25}$	$^{+3}_{-4}$	$^{+8}_{-5}$	$^{+4}_{-11}$	$^{+17}_{-7}$	$^{+24}_{-18}$	$^{+61}_{-26}$	$^{+13}_{-12}$	$^{+26}_{-23}$	$^{+55}_{-62}$	$^{+157}_{-87}$
$J/\psi \to \phi\eta$	-1	-10	0	$+2$	0	$+3$	$+11$	$+3$	-4	$+12$	$+16$	$+26$
Phase space description	0	$+3$	-1	-1	-1	0	-11	$+7$	-3	$+10$	$+38$	-21
Breit-Wigner formula	0	-6	$+1$	$+6$	-5	-5	$+15$	-58	$+2$	$+4$	$+20$	-18
Total	$^{+23}_{-74}$	$^{+28}_{-100}$	$^{+4}_{-10}$	$^{+16}_{-8}$	$^{+14}_{-25}$	$^{+32}_{-16}$	$^{+66}_{-57}$	$^{+88}_{-155}$	$^{+24}_{-36}$	$^{+70}_{-23}$	$^{+140}_{-63}$	$^{+165}_{-100}$

TABLE IV. Summary of the systematic error sources and their corresponding contributions to the branching fractions of $J/\psi \to \gamma X$, $X \to \eta\eta$ (%), which are denoted as $\Delta\mathcal{B}$.

Systematic error	$\Delta\mathcal{B}(f_0(1500))$	$\Delta\mathcal{B}(f_2'(1525))$	$\Delta\mathcal{B}(f_0(1710))$	$\Delta\mathcal{B}(f_2(1810))$	$\Delta\mathcal{B}(f_0(2100))$	$\Delta\mathcal{B}(f_2(2340))$
Event selection	± 8.3	± 8.3	± 8.3	± 8.3	± 8.3	± 8.3
Background uncertainty	$^{+20.6}_{-46.1}$	$^{+23.5}_{-34.8}$	$^{+35.4}_{-15.1}$	$^{+5.1}_{-34.5}$	$^{+46.8}_{-9.7}$	$^{+24.9}_{-0.9}$
Extra resonances	$^{+11.1}_{-56.3}$	$+21.9$	$^{+33.2}_{-23.9}$	$^{+20.3}_{-19.0}$	$^{+26.9}_{-16.2}$	$^{+6.0}_{-27.8}$
Resonance parameters	$^{+18.0}_{-41.6}$	$^{+21.6}_{-12.0}$	$^{+17.0}_{-8.0}$	$^{+58.2}_{-14.4}$	$^{+11.3}_{-11.1}$	$^{+24.3}_{-19.3}$
$J/\psi \to \phi\eta$	-7.1	$+0.6$	$+7.6$	-6.4	$+8.7$	$+5.0$
Phase space description	-1.6	-3.2	-0.5	$+10.7$	-1.0	$+21.1$
Breit-Wigner formula	-6.3	$+6.8$	-8.4	-4.9	-7.4	-12.5
Total	$^{+30.7}_{-84.8}$	$^{+40.2}_{-37.9}$	$^{+52.6}_{-31.7}$	$^{+63.3}_{-43.5}$	$^{+56.5}_{-24.6}$	$^{+42.3}_{-37.0}$

is taken to be the systematic error. Similarly the systematic error from η selection criteria is estimated to be 0.8%.

(iv) Number of J/ψ events. In the calculation of branching fractions, the number of J/ψ events, $(225.3 \pm 2.8) \times 10^6$ [9], determined from J/ψ inclusive hadronic decays, was used, and its uncertainty, 1.24%, is taken as the systematic error.

The systematic error sources and their contributions studied above are all summarized in Tables III and IV, in which the systematic error from event selection includes the contributions from photon detection efficiency, kinematic fit, η selection and the number of J/ψ events listed in Table II. The total systematic error is the sum of them added in quadrature.

VI. SUMMARY

Using 225 million J/ψ events collected with the BESIII detector, a PWA of $J/\psi \to \gamma\eta\eta$ has been performed, and the results are summarized in Table I. The scalar contributions are mainly from $f_0(1500)$, $f_0(1710)$ and $f_0(2100)$, while no evident contributions from $f_0(1370)$ and $f_0(1790)$ are seen. Recently, the production rate of the pure gauge scalar glueball in J/ψ radiative decays predicted by the lattice QCD [35] was found to be compatible with the production rate of J/ψ radiative decays to $f_0(1710)$; this suggests that $f_0(1710)$ has a larger overlap with the glueball compared to other glueball candidates [e.g., $f_0(1500)$]. In this analysis, the production rates of $f_0(1710)$ and $f_0(2100)$ are both about 1 order of magnitude larger than that of the $f_0(1500)$ and no clear evidence is found for $f_0(1370)$, which are both consistent with, or at least not contrary to, lattice QCD predictions.

Studies using data from $\bar{p}p$ annihilation [27,28] show that the $f_0(2100)$ has strong coupling to $\eta\eta$, but much weaker to $\pi\pi$, which indicates an exotic $f_0(2100)$ decay pattern. Searching for more decay modes of $f_0(2100)$ in J/ψ radiative decays may help to clarify its nature.

The tensor components, which are dominantly from $f_2'(1525)$, $f_2(1810)$ and $f_2(2340)$, also have a large contribution in $J/\psi \to \gamma\eta\eta$ decays. The significant contribution from $f_2'(1525)$ is shown as a clear peak in the $\eta\eta$ mass spectrum; a tensor component exists in the mass region from 1.8 GeV/c^2 to 2 GeV/c^2, although we cannot distinguish $f_2(1810)$ from $f_2(1910)$ or $f_2(1950)$; and the PWA requires a strong contribution from $f_2(2340)$, although the possibility of $f_2(2300)$ cannot be ruled out. For the narrow $f_J(2220)$, no evident peak is observed in the $\eta\eta$ mass spectrum. We have also tried to add it in the analysis, but its statistical significance is quite small, just 0.4σ.

ACKNOWLEDGMENTS

The BESIII collaboration thanks the staff of BEPCII and the computing center for their hard efforts. This work is supported in part by the Ministry of Science and Technology of China under Contract No. 2009CB825200; National Natural Science Foundation of China (NSFC) under Contracts No. 10625524, No. 10821063, No. 10825524, No. 10835001, No. 10935007, No. 11125525, and No. 11235011; Joint Funds of the National Natural Science Foundation of China under Contracts No. 11079008, and No. 11179007; the Chinese Academy of Sciences (CAS) Large-Scale Scientific Facility Program; CAS under Contracts No. KJCX2-YW-N29, and No. KJCX2-YW-N45; 100 Talents Program of CAS; German Research Foundation DFG under Contract Number Collaborative Research Center CRC-1044; Istituto Nazionale di Fisica Nucleare, Italy; Ministry of Development of Turkey under Contract No. DPT2006K-120470; U.S. Department of Energy under Contracts No. DE-FG02-04ER41291, No. DE-FG02-05ER41374, and No. DE-FG02-94ER40823; U.S. National Science Foundation; University of Groningen (RuG) and the Helmholtzzentrum fuer Schwerionenforschung GmbH (GSI), Darmstadt; WCU Program of National Research Foundation of Korea under Contract No. R32-2008-000-10155-0.

[1] F. E. Close, Rep. Prog. Phys. **51**, 833 (1988).
[2] S. Godfrey and J. Napolitano, Rev. Mod. Phys. **71**, 1411 (1999).
[3] C. Amsler and N. A. Tornqvist, Phys. Rep. **389**, 61 (2004).
[4] E. Klempt and A. Zaitsev, Phys. Rep. **454**, 1 (2007).
[5] V. Crede and C. A. Meyer, Prog. Part. Nucl. Phys. **63**, 74 (2009).
[6] Y. Chen *et al.*, Phys. Rev. D **73**, 014516 (2006).
[7] E. Gregory, A. Irving, B. Lucini, C. McNeile, A. Rago, C. Richards, and E. Rinaldi, J. High Energy Phys. 10 (2012) 170.
[8] C. Edwards *et al.*, Phys. Rev. Lett. **48**, 458 (1982).
[9] M. Ablikim *et al.* (BESIII Collaboration), Chinese Phys. C **36**, 915 (2012).
[10] J. Z. Bai *et al.* (BES Collaboration), Nucl. Instrum. Methods Phys. Res., Sect. A **344**, 319 (1994); **458**, 627 (2001).
[11] M. Ablikim *et al.* (BESIII Collaboration), Nucl. Instrum. Methods Phys. Res., Sect. A **614**, 345 (2010).
[12] S. Agostinelli *et al.* (GEANT4 Collaboration), Nucl. Instrum. Methods Phys. Res., Sect. A **506**, 250 (2003).
[13] S. Jadach, B. F. L. Ward, and Z. Was, Comput. Phys. Commun. **130**, 260 (2000).
[14] S. Jadach, B. F. L. Ward, and Z. Was, Phys. Rev. D **63**, 113009 (2001).
[15] R. G. Ping, M. Yan-Yun, Q. Xiu-Bo, Z. Zhe, C. Xing-Zhong, Y. Run-Sheng, and W. Bao-Yi, Chinese Phys. C **32**, 243 (2008).
[16] J. Beringer *et al.* (Particle Data Group), Phys. Rev. D **86**, 010001 (2012).
[17] J. C. Chen, G. S. Huang, X. R. Qi, D. H. Zhang, and Y. S. Zhu, Phys. Rev. D **62**, 034003 (2000).
[18] N. Berger, B. J. Liu, and J. K. Wang, J. Phys. Conf. Ser. **219**, 042031 (2010).
[19] B. S. Zou and D. V. Bugg, Eur. Phys. J. A **16**, 537 (2003).
[20] J. G. Korner, J. H. Kühn, and H. Schneider, Phys. Lett. **120B**, 444 (1983).
[21] S. N. Dymov, V. S. Kurbatov, I. N. Silin, and S. V. Yaschenko, Nucl. Instrum. Methods Phys. Res., Sect. A **440**, 431 (2000).
[22] We tested the following mesons listed in PDG 2012: $f_2(1270)$, $f_0(1370)$, $f_2(1430)$, $f_0(1500)$, $f_2'(1525)$, $f_2(1565)$, $f_2(1640)$, $f_0(1710)$, $f_2(1810)$, $f_2(1910)$, $f_2(1950)$, $f_2(2010)$, $f_0(2020)$, $f_4(2050)$, $f_0(2100)$, $f_2(2150)$, $f_0(2200)$, $f_J(2220)$, $f_2(2300)$, $f_4(2300)$, $f_0(2330)$, $f_2(2340)$.
[23] J. Z. Bai *et al.* (BES Collaboration), Phys. Rev. D **68**, 052003 (2003).
[24] M. Ablikim *et al.* (BES Collaboration), Phys. Lett. B **642**, 441 (2006).
[25] J. Z. Bai *et al.* (BES Collaboration), Phys. Lett. B **472**, 207 (2000).
[26] A. V. Anisovich *et al.*, Phys. Lett. B **449**, 145 (1999).
[27] A. V. Anisovich, C. A. Baker, C. J. Batty, D. V. Bugg, C. Hodd, H. C. Lu, V. A. Nikonov, A. V. Sarantsev, V. V. Sarantsev, and B. S. Zou, Phys. Lett. B **491**, 47 (2000).
[28] A. V. Anisovich *et al.*, Nucl. Phys. **A662**, 319 (2000).
[29] M. Ablikim *et al.* (BES Collaboration), Phys. Lett. B **607**, 243 (2005).
[30] R. M. Baltrusaitis *et al.* (MARKIII Collaboration), Phys. Rev. Lett. **56**, 107 (1986).
[31] J. Z. Bai *et al.* (BES Collaboration), Phys. Rev. Lett. **81**, 1179 (1998).
[32] J. H. Kuhn and A. Santamaria, Z. Phys. C **48**, 445 (1990).
[33] M. Ablikim *et al.* (BESIII Collaboration), Phys. Rev. D **83**, 112005 (2011).
[34] M. Ablikim *et al.* (BESIII Collaboration), Phys. Rev. D **81**, 052005 (2010).
[35] L. C. Gui, Y. Chen, G. Li, C. Liu, Y.-B. Liu, J.-P. Ma, Y.-B. Yang, and J.-B. Zhang, Phys. Rev. Lett. **110**, 021601 (2013).